

A Comparative Study of the Tension Estimation Methods for Cable Supported Bridges

Byeong Hwa Kim^{1,*}, Taehyo Park², Hyunyang Shin³ and Tae-Yang Yoon⁴

¹Ph.D., Steel Structure Research Laboratory, Research Institute of Industrial Science & Technology, 79-5, Youngcheon, Dongtan, Hwasung, Kyunggi, 445-813, Korea

²Associate Professor, Ph.D., Department of Civil Engineering, Hanyang University, 17 Haengdang-dong, Seoul, 133-791, Korea

³Ph.D., Department of Civil Engineering, Samsung Engineering & Construction, 263 Seohyun Bundang, Kyunggi, 463-721, Korea

⁴Ph.D., Steel Structure Research Laboratory, Research Institute of Industrial Science & Technology, 79-5, Youngcheon, Dongtan, Hwasung, Kyunggi, 445-813, Korea

Abstract

This paper presents a comparative field study of the available vibration-based tension estimation techniques for cable supported bridges. The various techniques have been applied to the four inclined stay-cables on the Seohae Grand Bridge and the seven double hangers on the Yeongjong Grand Bridge. The estimated tensions have been compared with those of static tests. For stay cables on cable-stayed bridges, it is seen that the accuracy of the estimation results is affected by the sag-to-span ratio and the bending stiffness of cables. For the hangers on suspension bridges, the clamp location ratio and the effective length are the critical factors that affect the accuracy of the estimation results. Among the various techniques, the frequency-based system identification technique shows a consistent estimation error bound of 3% for a wide range of applications.

Keywords: cable tension; cable dynamics; hanger cable; suspension bridge; system identification

1. Introduction

In these days, constructing long span bridges is a growing trend, and the record-breaking long span bridges are frequently introduced. These accomplishments are attributed to modern advances in material, analysis, and construction technology. Especially, the emergence of high strength cables plays an important role in winning a great popularity of cable supported bridges. Since cables are a crucial element for the overall structural safety of such structures, the accurate estimation of tension force is of major importance on both the construction and the maintenance stages of the stays and hangers.

The two categories of techniques are available for monitoring cable tension. One is the static method that directly measures the cable tension by pre-installed load cells or by the lift-off hydraulic jacks. While the calibrated load cell can be monitored over relatively long period of time, the durability of the sensors is somewhat limited comparing to the service life of cables. In addition, the initial costs of the load cells have frequently influenced on decision of their use. The lift-off technique using a hydraulic jack is very expensive for larger cables because

of the high strength needed. The lift-off technique also involves removal of parts of anchorage system. The other category is the vibration-based method that indirectly estimates the tension force using the measured natural frequencies. The vibration method is often used by field engineers because it provides an efficient, cheap and relatively easy way to determine the cable forces.

The typical procedures of the vibration methods are as follows. First, the time responses of cable are collected by a data logger for the excitation of an impact hammer, or ambient sources such as normal traffic loads and winds. Next, the natural frequencies and mode numbers are extracted by various modal analysis techniques for the collected data sets. Finally, the tension forces are determined by using an appropriate analytical closed-form or numerical algorithm-form relationship between natural frequencies and cable tension.

The objective of this paper is to investigate the performance of the existing vibration-based methods through real cable-supported bridges. To achieve the objective, the following three tasks are performed. First, the fundamental principles of the existing various vibration methods have been revisited. Second, the performance of the methods has been examined via the inclined stay-cables on Seohae cable-stayed bridge and the double hanger systems on Yeongjong suspension bridges. Third, the results are compared and some conclusions are made.

*Corresponding author

Tel: 82-31-370-9643; Fax: 82-31-370-9599

E-mail: bhk1272@rist.re.kr

2. Available Vibration-based Methods

The relationship between frequencies and cable tension may be classified as the following four classes, according to the consideration of the sag-extensibility and bending stiffness of a cable. The first class utilizes the flat taut string theory that neglects both sag-extensibility and bending stiffness of the cable:

$$T = 4mL^2 \left(\frac{f_n}{n} \right)^2 \quad (1)$$

where T , m , L , and f_n denote cable tension, mass density, length of cable, and the n th natural frequency, respectively. The tension force can be easily determined from measuring the system variables in the left hand side of Eq. (1). However, this simple formula is only valid for a flat long slender single cable. Although Eq. (1) is unreliable for cables with high sag, high bending stiffness, and a double hanger system, it is helpful for the first approximation of tension.

The second class makes use of the following frequency formula of an axially loaded beam that takes account of the bending effect without sag-extensibility (Shimada *et al.*, 1989):

$$\left(\frac{f_n}{n} \right)^2 = \left(\frac{1}{4mL^2} \right) T + \left(\frac{n^2 \pi^2}{4mL^4} \right) EI \quad (2)$$

where EI denotes the flexural rigidity of a cable. With respect to the unknown tension force and flexural rigidity, the linear regression procedures are applied to the measured frequencies and the corresponding mode numbers. Hence, the flexural rigidity and tension can be simultaneously estimated. Although the estimated results are very reliable for a short thick single cable, the estimated flexural rigidity is unreliable for the high sagged cables. Furthermore, the utilization of higher modes provides better accuracy while the higher modes of a large cable are hardly excited by the ambient sources. Despite those limitations, this approach is often used in the field due to its simplicity and speediness.

Third category uses the modern cable theory (Triantafyllou and Grinfolgel 1986) that considers the sag-extensibility without bending stiffness:

$$\sin(\gamma) \left[\gamma \left(\frac{4\gamma^2}{\lambda_1^2} - 1 \right) \cos(\gamma) + \sin(\gamma) \right] - \frac{49}{64} \frac{\varepsilon^2}{1 + \left(\frac{l}{h} \right)^2} \cos(2\gamma) = 0 \quad (3)$$

where, $\gamma = (\omega_n L_s / 2) \sqrt{m/T_a}$; $T_a = H/\cos(\theta)$; $\lambda_1^2 = (wL_s/T_a)^2 EA/T_a \cos^2(\theta)$; $\varepsilon = wL_s/T_a$; $\omega_n = 2\pi f_n$.

The variables H , w , EA , θ , h , l , and L_s are the horizontal component of tension, the weight per unit length, the axial rigidity, angle between the cable cord and the horizontal, the height, the horizontal span, and initial unstrained length of a sagged elastic single cable,

respectively. Given the measured frequencies, this nonlinear characteristic Eq. (3) is solved by the trial-and-error method for the horizontal component of tension (Russell and Lardner 1998). However, Eq. (3) requires a priori knowledge regarding the axial rigidity and the unstrained length of cable that is often not available in practice.

The last category includes two different approaches that take account of both sag-extensibility and bending stiffness. One is the traditional approach that uses the following approximate analytical closed-form practical formulas (Zui *et al.*, 1996):

In the case that a cable has small sag ($3 \leq \Gamma$),

$$T = 4m(f_1 L)^2 \left[1 - 2.2 \frac{C}{f_1} - 0.55 \left(\frac{C}{f_1} \right)^2 \right]; \quad (17 \leq \xi_1) \quad (4)$$

$$T = 4m(f_1 L)^2 \left[0.865 - 11.6 \left(\frac{C}{f_1} \right)^2 \right]; \quad (6 \leq \xi_1 \leq 17) \quad (5)$$

$$T = 4m(f_1 L)^2 \left[0.828 - 10.5 \left(\frac{C}{f_1} \right)^2 \right]; \quad (0 \leq \xi_1 \leq 6) \quad (6)$$

In the case that a cable has large sag ($\Gamma \leq 3$),

$$T = m(f_2 L)^2 \left[1 - 4.40 \frac{C}{f_2} - 1.10 \left(\frac{C}{f_2} \right)^2 \right]; \quad (60 \leq \xi_1) \quad (7)$$

$$T = m(f_2 L)^2 \left[1.03 - 6.33 \frac{C}{f_2} - 1.58 \left(\frac{C}{f_2} \right)^2 \right]; \quad (17 \leq \xi_1 \leq 60) \quad (8)$$

$$T = m(f_2 L)^2 \left[0.882 - 85.0 \left(\frac{C}{f_2} \right)^2 \right]; \quad (0 \leq \xi_1 \leq 17) \quad (9)$$

In the case that the higher modes are used,

$$T = \frac{4m}{n^2} (f_n L)^2 \left(1 - 2.20 \frac{nC}{f_n} \right); \quad (200 \leq \xi_1), \quad (2 \leq n) \quad (10)$$

where, $C = \sqrt{(EI)/(mL^4)}$; $\xi_1 = \sqrt{T/EI} \cdot L$;

$$\Gamma = \sqrt{(wL)/(128EA\delta^3 \cos^5 \theta)} \left[\frac{0.31\xi_1 + 0.5}{0.31\xi_1 - 0.5} \right];$$

δ = sag-to-span ratio. The determination of tension is straightforward for the given measured modes, the sag-to-span ratio of cable, the flexural rigidity, and axial rigidity. However, the sag-to-span ratio is often not available in practice because measuring the static shape of cable needs high cost. In addition, the flexural rigidity and axial rigidity of an elastic cable are often unavailable or invalid in some practical cases. For instance, the shear and bending mechanisms of a cable element may not be the same with those of a continuum structure because the cross section of the most structural cables consists of individual strands.

The other approach of the last category is the state-of-the-art system identification method that identifies a finite element model whose modes are identical to the

measured frequencies using a sensitivity updating algorithm (Park and Kim 2005, Kim and Park 2005). The algorithm consists of the following five steps. First, the identification variable vector \mathbf{U} including the cable tension is defined, and its initial values are assumed. Second, the sensitivity matrix \mathbf{F} is approximated using the finite element analysis:

$$\mathbf{F} = \begin{bmatrix} \frac{\partial \beta_1 U_1}{\partial U_1 \beta_1} & \cdots & \frac{\partial \beta_1 U_p}{\partial U_p \beta_1} \\ \frac{\partial \beta_q U_1}{\partial U_1 \beta_q} & \cdots & \frac{\partial \beta_q U_p}{\partial U_p \beta_q} \end{bmatrix} \quad (11)$$

where, β_i and U_i denote the i th eigenvalue and the i th item of \mathbf{U} , respectively. The subscript p and q denote the number of identification variables and the number of measured natural frequencies, respectively. Third, the variations of eigenvalue \mathbf{Z} are obtained with respect to the measured target eigenvalues:

$$\mathbf{Z} = \left[\frac{\beta'_1 - \beta_1^k}{\beta_1^k} \cdots \frac{\beta'_n - \beta_n^k}{\beta_n^k} \cdots \frac{\beta'_q - \beta_q^k}{\beta_q^k} \right]^T \quad (12)$$

where, the superscript β'_n and β_n^k denote the n th measured target eigenvalue and the n th eigenvalue of the finite element model computed at the step of the k th iteration, respectively. Fourth, the fractional changes in the identification variables α are determined by

$$\alpha = \mathbf{F}^{-1} \mathbf{Z} \quad (13)$$

Finally, the identification variables are updated by

$$U_i^{k+1} = (1 + \alpha_i^k) U_i^k \quad (14)$$

where, U_i^k denotes the i th identification variable of \mathbf{U} at the step of the k th iteration, and α_i denotes the i th element of α at the step of the k th iteration. These steps are repeated until the fractional changes of the identification variable α_i converge to zeros. Although the algorithm is quite involved, the technique can be applied to a wide range of cable structures because the relation between frequencies and tension is obtained by a finite element analysis, instead of the typical closed-form analytical solution. In addition, this approach does not require information regarding the material properties such as the bending rigidity, axial rigidity, sag-to-span ratio, and unstrained length of cables. Hence, this frequency-based tension identification approach is most promising in practical use.

For a single stay-cable on cable-stayed bridges, all of the aforementioned five categories could be applied with some reasonable assumptions. However, the nonlinear characteristic equation of the sagged single cable in the third category and the practical formula in the last category may not be valid for a typical double hanger system on suspension bridges that consists of two independent



Figure 1. Seohae cable-stayed bridge.

Table 1. Dimensions of the stay-cable No. 1 and No. 44 on the Seohae cable-stayed bridge

| Dimensions | Stay-cable No. 1 | Stay-cable No. 44 |
|------------------------------|---------------------|---------------------|
| Horizontal span l | 200.68 m | 131.3 m |
| Height h | 110.03 m | 90.57 m |
| Self weight w | 1226.25 N/m | 794.61 N/m |
| Angle to Horizontal θ | 27.74° | 33.22° |
| Wires | 91 × ϕ 15.7 mm | 61 × ϕ 15.7 mm |

cables tied by a clamp and a spacer. The reason is that the accurate analytical closed-form solutions are unknown, and the sag-extensibility of the hangers can be negligible due to their verticality and straightness.

3. Field Study

3.1 Stay-cables on cable-stayed bridges

Rising above the Asan Bay approximately 65 km south of Seoul, the Seohae cable-stayed bridge, built in 2000, is a part of the 7.31 km long highway linking Seoul and Mokpo. As shown in Fig. 1, the bridge is 990 m long and it has total 144 stay-cables. The 24 accelerometers are attached to the specific stay-cables (Park *et al.*, 2004) for the on-line health monitoring. Here, the total four sets of time history data collected from the No. 1 and No. 44 cables for each direction of Seoul and Mokpo are considered. The dimensions of the test structures are shown in Table 1. The cable No. 1 is the longest cable and it is the weakest one for vibration. It is also reported that the time history data collected from the cable No. 44 has the worst quality.

For the wind excitation (an average velocity of 4.23 m/s) and the normal traffic conditions, the acceleration time responses of cables are obtained by piezoelectric-type accelerometers with the sampling rate of 0.01 sec for 10 minutes. The typical power spectrum density (NFFT = 2048, Hanning window) of the cable No.1 for the Seoul direction is shown in Fig. 2. As shown in Table 2, the lower 30 and 20 modes of the cable No.1 and No.44, respectively, are extracted by the time domain decomposition technique (Kim *et al.*, 2005) and the Eigen-system realization algorithm with data correlation techniques

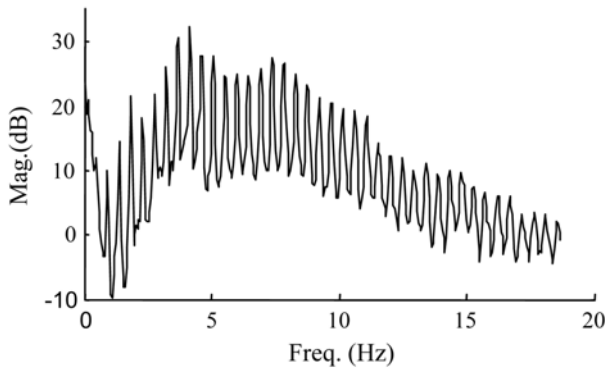


Figure 2. Spectrum of acceleration collected from the stay-cable No. 1 toward Seoul.

Table 2. Measured natural frequencies (Hz) of the stay-cables on Seohae cable-stayed bridge

| Mode | Stay-cable No. 1 | | Stay-cable No. 44 | |
|------|------------------|-------|-------------------|-------|
| | Seoul | Mokpo | Seoul | Mokpo |
| 1 | (0.47) | - | - | - |
| 2 | 0.94 | 0.92 | 1.50 | 1.51 |
| 3 | 1.38 | 1.38 | 2.26 | 2.27 |
| 4 | 1.84 | 1.84 | 3.01 | 3.02 |
| 5 | 2.30 | 2.29 | 3.77 | 3.78 |
| 6 | 2.76 | 2.75 | 4.52 | 4.55 |
| 7 | 3.23 | 3.21 | 5.29 | 5.31 |
| 8 | 3.69 | 3.67 | 6.03 | 6.05 |
| 9 | 4.15 | 4.13 | 6.79 | 6.82 |
| 10 | 4.61 | 4.59 | 7.55 | 7.585 |
| 11 | 5.08 | 5.05 | 8.31 | 8.33 |
| 12 | 5.54 | 5.51 | 9.06 | 9.09 |
| 13 | 6.00 | 5.98 | 9.81 | 9.83 |
| 14 | 6.46 | 6.44 | 10.58 | 10.61 |
| 15 | 6.93 | 6.89 | 11.34 | 11.34 |
| 16 | 7.39 | 7.35 | 12.06 | 12.09 |
| 17 | 7.85 | 7.81 | 12.83 | 12.84 |
| 18 | 8.31 | 8.28 | 13.59 | 13.58 |
| 19 | 8.76 | 8.73 | 14.35 | 14.30 |
| 20 | 9.24 | 9.19 | 15.10 | 15.10 |
| 21 | 9.69 | 9.64 | - | - |
| 22 | 10.16 | 10.10 | - | - |
| 23 | 10.63 | 10.57 | - | - |
| 24 | 11.07 | 11.03 | - | - |
| 25 | 11.55 | 11.52 | - | - |
| 26 | 12.03 | 11.95 | - | - |
| 27 | 12.49 | 12.44 | - | - |
| 28 | 12.94 | 12.90 | - | - |
| 29 | 13.42 | 13.35 | - | - |
| 30 | 13.89 | 13.82 | - | - |

(Juang 1992). Normally speaking, those statistical modal parameter estimation methods significantly reduce uncertainty on the estimation of modal parameters, compared to the Pick-picking method. Here, the first lower modes of the cable No. 1 and No. 44 were not measured.

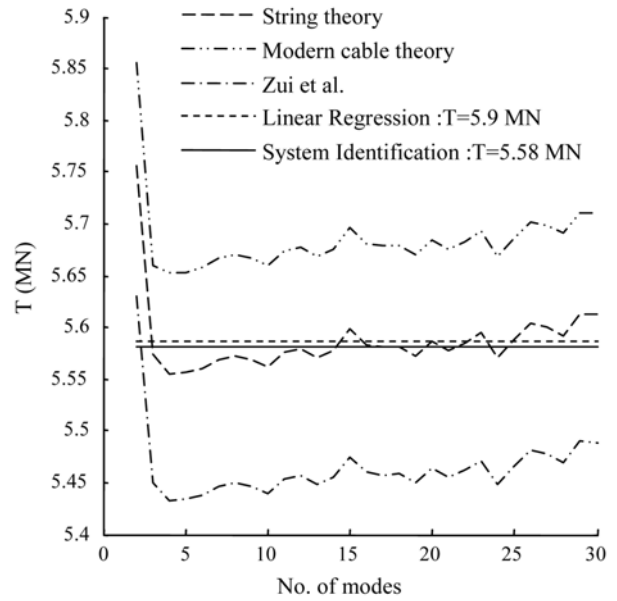


Figure 3. Estimated tensions of stay-cable No.1 in the direction of Seoul.

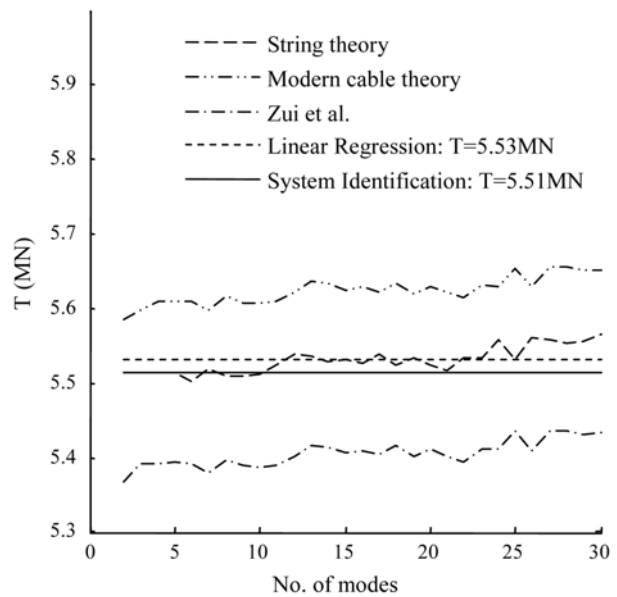


Figure 4. Estimated tensions of stay-cable No. 1 in the direction of Mokpo.

For the measured modes of the stay cables, the existing five methods are applied to estimate tension forces. As shown in Fig. 3-5, the estimated tensions for each mode are similar to those computed by the string theory in Eq. (1), the modern cable theory in Eq. (3), and the practical formula in Eq. (10). In addition, the practical formula and the modern cable theory tend to show the lower and the upper bounds. The reason may be due to insufficient information regarding the axial rigidity, unstrained length of cable, and the sag-to-span ratio. Meanwhile, the tensions computed by the string theory are very similar to those by the linear regression approach and by the system

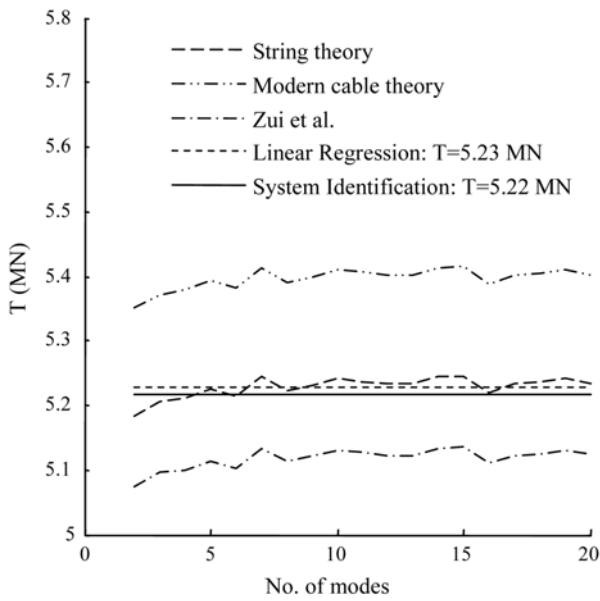


Figure 5. Estimated tensions of stay-cable No.44 in the direction of Seoul.

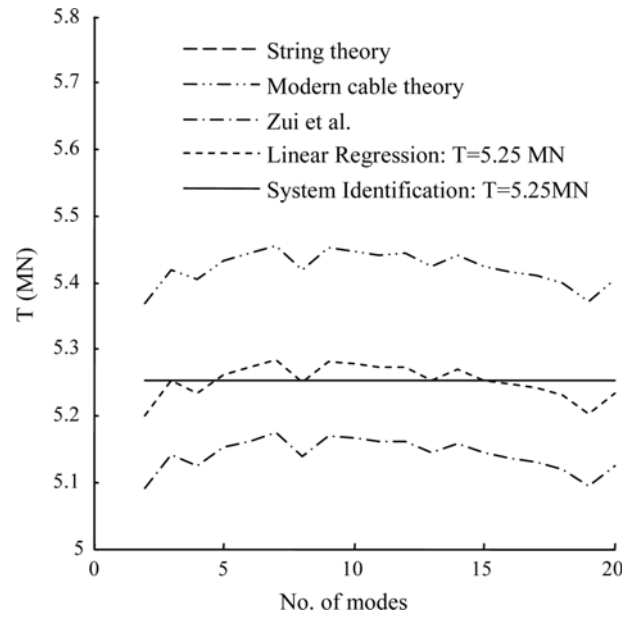


Figure 6. Estimated tensions of stay-cable No.44 in the direction of Mokpo.

identification approach. Here, the first four lower modes are neglected in the linear regression method because the sag-extensibility mainly affects lower modes. In Fig. 3, the variation of the resulting tensions for the second mode is relatively high in some categories of methods such as the string theory, the modern cable theory, and practical formula. The reason may be due to the negligence of the bending stiffness of the cable. The averaged values of the resulting tensions are shown in Table 3. The first row indicates the tensions measured by the lift-off method using a tensioning hydraulic jack at August in 2001 (Park *et al.*, 2004). The parenthesis in Table 3 shows the percentile errors of the estimated tension forces with respect to those of the lift-off method. All the estimated tension forces show very good agreements. This is because the cable system considered here has very small sag and low bending stiffness due to the high level of tension force. It is particularly seen that the system identification approach and the linear regression approach show a consistent estimation error of the 3% bound for the selected range of applications.

3.2 Hangers on suspension bridges

The Yongjong bridge, built in 2000, is a part of the 40.2 km long Incheon International Airport Highway in Korea. The self-anchored suspension bridge is 550 m long as shown in Fig. 7. The bridge span consists of the center span of 300 m and side spans of 125 m. The two main cables of the bridge curve three-dimensionally from the top of each diamond-shaped tower to the outside of the stiffening girder at the main span. To transfer the traffic loads on the stiffening girder into the main cables, total 43 hanger cable systems are installed on each main cable. Each hanger system consists of two pairs of the inclined double hanger cables tied by a clamp as shown in Fig. 8.

Ambient vibration tests have been conducted for the seven sets of the double hanger systems (NTS03~NTS09) on the north side in the direction of the airport. The nominal diameter and mass of a single hanger cable is $\phi 8.4 \times 10^{-2}$ m and 32.4 kg/m, respectively. The dimensions of the hangers are shown in Table 4. The first column in Table 4 indicates the length between the center of main cable and the deck plate. The symbol h in the second

Table 3. Estimated tensions (MN) for the stay-cables

| Applied methods | Stay-cable No. 1 | | Stay-cable No. 1 | |
|--------------------------------|------------------|------------|------------------|-------------|
| | Seoul | Mokpo | Seoul | Mokpo |
| The lift-off method | 5.64 | 5.61 | 5.31 | 5.19 |
| String theory (Eq. 1) | 5.59 (0.9) | 5.53 (1.4) | 5.23 (1.5) | 5.25 (-1.2) |
| Linear regression (Eq. 2) | 5.57 (1.3) | 5.51 (1.8) | 5.23 (1.5) | 5.28 (-1.7) |
| Modern cable theory (Eq. 3) | 5.68 (-0.7) | 5.62 (1.6) | 5.40 (-1.7) | 5.42 (-4.4) |
| Practical formula (Eq. 10) | 5.46 (3.2) | 5.41 (3.6) | 5.12 (3.6) | 5.14 (1.0) |
| System Identification (Eq. 14) | 5.59 (0.9) | 5.53 (1.4) | 5.23 (1.5) | 5.25 (-1.2) |

Note: () is % error with respect to the lift-off method.



Figure 7. Yongjong suspension bridge.



Figure 8. Double hanger system (NTS03).

column of Table 4 denotes the clamp location which is the length from the center of main cable to the center of the horizontal clamp. Here, the clamp location h of the bridge is 1.1 m for all the hanger systems considered. Hence, it is expected that the clamp may severely affect on the dynamic behavior of the shortest hanger cable system NTS03, while the effect of the clamp on the longest hanger cable system NTS09 may be negligible. The symbol B and q in Table 4 denote the width between the two individual hanger cables and angles between hanger cables and the horizontal, respectively. For normal traffic excitations on the stiffening girder, the acceleration time responses of the hanger cables had been collected. Using three accelerometers on hangers, the roving sensor technique was conducted in this modal test of the double hanger cable systems. The sampling rate of the data logger was set to 500 Hz. The power spectrum density

Table 4. Dimensions of the double hanger system on the Yongjong suspension bridge

| Hanger No | Length L (m) | Ratio h/L (%) | Width B (m) | Angle θ (deg) |
|-----------|-------------------|--------------------|------------------|-------------------------|
| NTS03 | 2.87 | 38.3 | 0.62 | 4.67 |
| NTS04 | 7.37 | 14.9 | 0.76 | 11.04 |
| NTS05 | 12.83 | 8.6 | 0.76 | 12.30 |
| NTS06 | 19.14 | 5.7 | 0.76 | 12.68 |
| NTS07 | 26.33 | 4.2 | 0.76 | 12.81 |
| NTS08 | 34.41 | 3.2 | 0.76 | 12.83 |
| NTS09 | 43.36 | 2.5 | 0.76 | 12.80 |

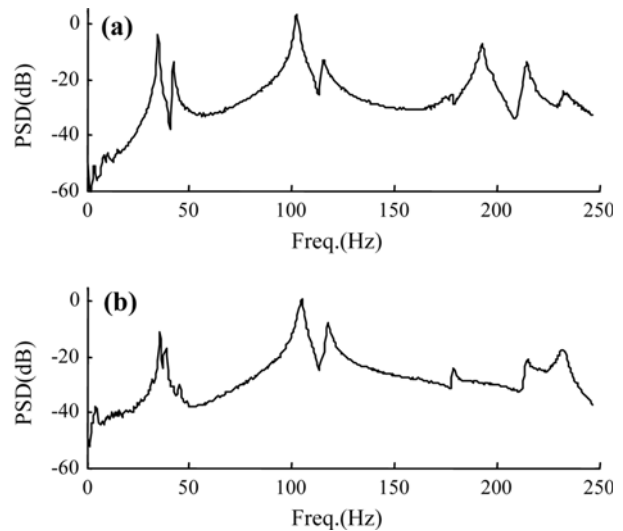


Figure 9. Power spectrum of the hanger cable NTS03: (a) in the x direction; (b) in the y direction.

(NFFT = 1024, Hanning window) of the hanger cable NTS03 is shown in Fig. 9. It is seen that there exists a pair of modes in each direction made of in-phase mode and out-of-phase mode. All the measured frequencies are shown in Table 5. Here, the directions, denoted by x and y , indicate the parallel and perpendicular directions of the longitudinal bridge axis, respectively. The gap between the two companion modes becomes smaller as the clamp location h becomes smaller. When the clamp location goes to zero, the frequencies of the double hanger system approach those of a single taut string theory. Hence, the four similar frequencies are closely-placed for the hanger cable system NTS09 in two measured directions. In order to distinguish modes and examine the boundary conditions of the hanger systems, the mode shapes of NTS03 are extracted using the time domain decomposition techniques (Kim *et al.*, 2005). The six and three mode shapes in the direction of x and y , respectively, are shown in Fig. 10. Here, the horizontal axis denotes the distance along the axial direction of the hanger cable. The first and last sensors locate below 0.2 m from the center of the main cable, and above 0.6 m from the deck plate, respectively. From the mode shapes, one can readily sure that the

Table 5. The measured natural frequencies (Hz) of the hanger systems on Yongjong suspension bridge

| | NTS03 | | NTS04 | | NTS05 | | NTS06 | | NTS07 | | NTS08 | | NTS09 | |
|----|--------|--------|--------|-------|-------|-------|-------|-------|-------|-------|-------|-------|-------|-------|
| | x | y | x | y | x | y | x | y | x | y | x | y | x | y |
| 1 | 34.79 | 35.65 | 13.55 | 13.67 | 7.07 | 7.15 | 4.53 | 4.63 | 3.52 | 3.59 | 2.26 | 2.52 | 1.78 | 1.71 |
| 2 | 42.36 | 104.98 | 14.28 | 16.97 | 7.19 | 7.81 | 4.69 | 4.84 | 3.67 | 3.77 | 2.32 | 2.64 | 1.84 | 1.88 |
| 3 | 102.54 | 118.16 | 25.76 | 25.63 | 14.08 | 14.18 | 9.08 | 9.32 | 7.05 | 7.23 | 4.57 | 4.65 | 3.57 | 3.61 |
| 4 | 115.2 | 214.2 | 27.47 | 36.01 | 14.41 | 16.02 | 9.39 | 9.79 | 7.34 | 7.56 | 4.65 | 5.08 | 3.68 | 3.76 |
| 5 | 193.0 | 232.4 | 40.65 | 41.26 | 21.02 | 21.06 | 13.73 | 13.98 | 10.64 | 10.90 | 6.88 | 7.03 | 5.40 | 5.47 |
| 6 | 222.4 | | 42.60 | 58.6 | 21.64 | | 14.18 | 14.86 | 11.07 | 11.41 | 7.04 | 7.64 | 5.55 | 5.66 |
| 7 | | | 61.52 | 63.72 | 28.32 | | 18.50 | 18.57 | 14.26 | 14.45 | 9.22 | 9.41 | 7.21 | 7.32 |
| 8 | | | 64.33 | 84.48 | 29.16 | | 19.00 | 19.75 | 14.84 | 15.37 | 9.39 | 10.23 | 7.40 | 7.52 |
| 9 | | | 87.52 | 91.92 | 37.01 | | 23.30 | | 17.91 | | 11.62 | 11.86 | 9.06 | 9.18 |
| 10 | | | 90.70 | | 38.05 | | 23.90 | | 18.67 | | 11.88 | 12.89 | 9.36 | 9.47 |
| 11 | | | 116.7 | | | | | | | | | | 10.96 | 11.08 |
| 12 | | | 121.09 | | | | | | | | | | 11.25 | 11.43 |
| 13 | | | | | | | | | | | | | 12.89 | 13.04 |
| 14 | | | | | | | | | | | | | 13.24 | 13.48 |
| 15 | | | | | | | | | | | | | 14.80 | 15.19 |
| 16 | | | | | | | | | | | | | 15.16 | 15.53 |

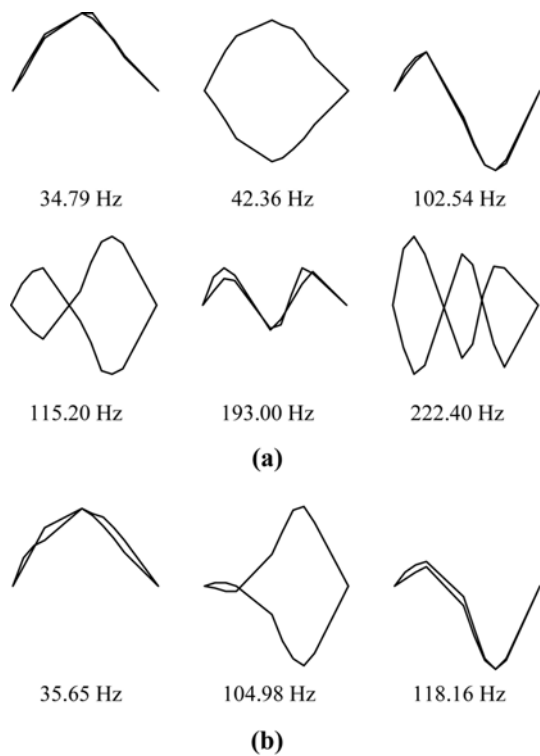


Figure 10. Mode shapes of the hanger cable system NTS03: (a) in the x direction; (b) in the y direction.

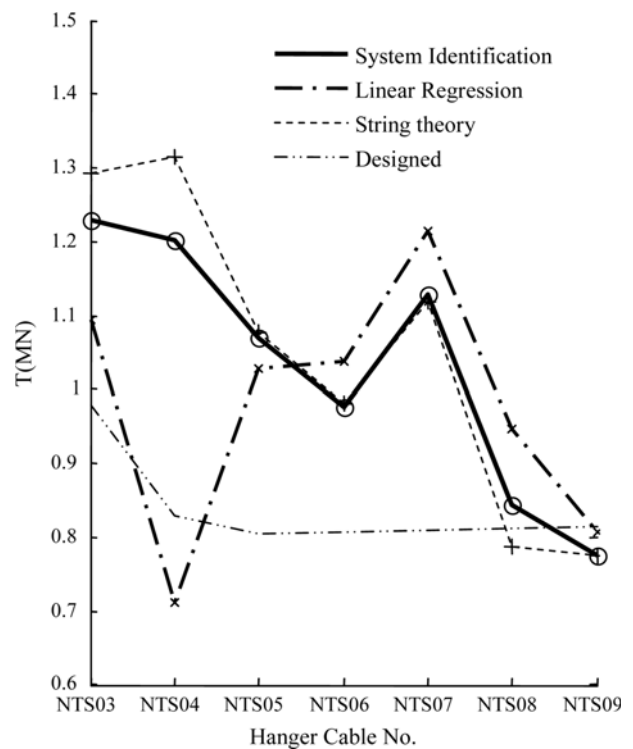


Figure 11. Estimated tension of the double hanger cable systems on Yongjong Bridge.

boundary conditions of the cable system near the deck plate can be modeled as a roller support.

For the measured modes, the tensions of the double hanger systems are estimated by the available methods such as the system identification method, the string theory, and the linear regression method. On the application of the string theory, only the first modes in the direction of

x are used because the first mode shapes are most similar to those of the taut string. In Fig. 11, the estimated tensions by the linear regression method come from by the New Airport HIWAY (Yong *et al.*, 2001). In this report, the authors pointed out that it is difficult to decide the effective length of the double hanger system because the individual cable length is unclear due to the clamp

and the deck plate. Thus, this previous estimation task was conducted for the two cases of the effective lengths. One is from the clamp to the hanger socket, and the other is from the clamp to the deck plate. The results shown in Fig. 11 are the later case. For a long hanger cable system such as NTS08 and NTS09, the effect of the clamp and the deck plate is negligible while the effect becomes severer in a short hanger cable system such as NTS03 and NTS04. However, this study proposes that the effective length for Eq. (2) should be counted from the center of the main cable to the deck plate with only the in-phase frequencies in the x direction. This is because the deck plate plays the role as a roller support and the deflection shapes in the x direction is much closer to those of a single straight cable as shown in Fig. 10. For the hanger system NTS03, the proposed effective length is accidentally similar to that between the clamp and the socket. This is the reason that there is a little difference between the estimated tensions by the system identification approach and the linear regression technique except the case of NTS03.

The estimated tensions show that the shorter hangers bear more tension than the longer hangers except the hanger system NTS07. In additions, the estimated tensions of NTS04 by the system identification technique have the maximum 40% and 31% differences from those of the linear regression method and the designed values, respectively. It is concluded that the system identification approach is particularly recommended to the accurate tension estimation of such double hanger system tied by a transverse connector.

4. Summary and Conclusions

The objective of this work is to introduce a comparative study of the existing vibration-based tension estimation methods. Firstly, the available vibration-based tension estimation methods were introduced and their application limits were reexamined. Next, the various existing methods were applied to the four stay-cables on the Seohae cable-stayed bridge and the four double hanger systems on the Yeongjong suspension bridge. Finally, the feasibility of the methods was compared.

Based on results and interpretations, the following three conclusions can be made. First, the system identification approach among the various methods has the most wide application range with reasonable accuracy. Second, the string theory is a good tool for the first approximation due to its simplicity and speediness. Third, a care should be

taken in the application of the linear regression method to a short hanger system.

Acknowledgments

The authors gratefully acknowledge the final support by Samsung Engineering & Construction. The authors also truly appreciate that Korean Highway Corporation and New Airport HIWAY have granted us permission to use the field data collected from Seohae cable-stayed bridge and Yeongjong grand bridge, respectively.

References

- Juang, J.-N. (1992). *Applied System Identification*, Prentice Hall, Englewood Cliffs, MJ.
- Kim, B.H. and Park, T. (2005). "Estimation of Cable Tension Using System Identification Technique: II. Experiments and Applications." *Korean Society of Civil Engineers Journal*, 25(4A), pp. 669-675.
- Kim, B.H., Stubbs, N. and Park, T. (2005). "A New method to extract modal parameters using output-only responses." *Journal of Sound and Vibration*, 282, pp. 215-230.
- Park, T. and Kim, B.H. (2005). "Estimation of cable tension using system identification technique: I. Theory." *Korean Society of Civil Engineers Journal*, 25(4A), pp. 661-668.
- Park, J.C., Park, C.M. and Song, P.Y. (2004). "Evaluation of structural behaviors using full scale measurements on the Seohae Cable-Stayed Bridge." *Korean Society of Civil Engineers*, 24(2A), 2004, pp. 249-257 (in Koreans).
- Russell, J.C. and Lardner, T.J. (1998). "Experimental determination of frequencies and tension for elastic cables." *Journal of Engineering Mechanics*, ASCE, 124(10), pp. 1067-1072.
- Shimada, T., Kimoto, K. and Narui, S. (1989). "Study on estimating tension of tied hanger rope of suspension bridge by vibration method." *Proc. JSCE*, 404(I-11), pp. 455-458.
- Triantafyllou, M.S. and Grinfogel, L. (1986). "Natural frequencies and modes of inclined cables." *Journal of Structural Engineering*, ASCE, 112(1), pp. 139-148.
- Yong, H.S. *et al.* (2001). "Safety inspection and structural stability evaluation for bridge maintenances on the Incheon International Airport Expressway." New Airport HIWAY®.
- Zui, H., Shinke T. and Namita Y.H. (1996). "Practical formulas for estimation of cable tension by vibration method." *Journal of Structural Engineering*, ASCE, 122(6), pp. 651-656.